Article

Discovery Medicine 2025; 37(194): 503–514
https://doi.org/10.24976/Discov.Med.202537194.42

Targeting HSF1-TLR9 Axis: Celastrol as a Potential Therapeutic for Liver Injury in Traumatic Hemorrhagic Shock

Jinjiang Zhu[1,†], Xiaoyun Sun[2,†], Yakun Zhan[3,*]

[1]Department of Emergency, Yiwu Central Hospital, 322000 Yiwu, Zhejiang, China
[2]Department of Pharmacy, The Eighth Hospital of Wuhan, 430014 Wuhan, Hubei, China
[3]Department of Emergency and Critical Care Medicine, The Second Affiliated Hospital, Jiangxi Medical College, Nanchang University, 330000 Nanchang, Jiangxi, China
*Correspondence: zhanyakun_zyku@163.com (Yakun Zhan)
[†]These authors contributed equally.
Published: 20 March 2025

Background: One of the pharmacological effects of celastrol (Cel) is the amelioration of acute liver injury. In this study, we explored the mechanism of Cel underlying the alleviation of liver injury induced by traumatic hemorrhagic shock (THS).
Methods: The THS model was developed from Sprague–Dawley rats through transverse fractures, blood loss and fluid infusion. Then, the THS rats were intraperitoneally injected with 0.5, 1, and 1.5 mg/kg Cel. The rats were injected in the tail vein with lentivirus-mediated small interfering RNA (siRNA) negative control (siNC), siRNA targeting heat shock transcription factor 1 (*siHSF1*), and siRNA targeting toll-like receptor 9 (*siTLR9*) 72 hours before the establishment of THS model. Hematoxylin-eosin (HE) staining was performed to highlight the pathological alterations in the rat liver tissue. Enzyme-linked immunosorbent Assay (ELISA) was utilized to determine the expression levels of alanine aminotransferase (ALT), aspartate aminotransferase (AST), tumor necrosis factor-alpha (TNF-α), interleukin-1 beta (IL-1β), and total bilirubin (TB). The expression levels of B-cell lymphoma 2 (*Bcl2*) and B-cell lymphoma 2 associated X protein (*Bax*) were evaluated by quantitative real-time polymerase chain reaction (qRT-PCR). The expression levels of reactive oxygen species (ROS), malondialdehyde (MDA), glutathione (GSH), and superoxide dismutase (SOD) were determined to assess the extent of oxidative stress. Western blotting was used to evaluate the expression levels of heat shock transcription factor 1 (HSF1), toll-like receptor 9 (TLR9) and myeloid differentiation factor 88 (MyD88).
Results: Cel was shown to therapeutically alleviate liver injury, decrease ALT and AST levels, and simultaneously downregulate inflammation factors levels (TNF-α, IL-1β), alleviated apoptosis, and decreased oxidative stress in the THS model in a concentration-dependent manner. Moreover, Cel increased the expression of *HSF1* and decreased the expression of *TLR9* and *MyD88* in the THS model. And silencing *HSF1* increased *TLR9* and *MyD88* expression. Further, the silencing of *HSF1* resulted in liver injury, inflammation and apoptosis, which could be reversed by *TLR9* silencing.
Conclusions: This study demonstrates that Cel attenuates THS-induced liver injury by positively regulating *HSF1* so as to inhibit the expression of *TLR9*.

Keywords: traumatic hemorrhagic shock; celastrol; liver injury; heat shock transcription factor 1; toll-like receptor 9; myeloid differentiation factor 88

Introduction

Traumatic hemorrhagic shock (THS) is the leading cause of mortality in patients after experiencing severe trauma, which is accompanied by multi-organ failure [1]. THS is associated with trauma of tissue and hemorrhagic shock [2]. In addition, acute liver injury, hepatic ischemia, and metabolic disorders of hepatocytes are commonplace among THS patients [3,4]. The pathological mechanisms driving the development of THS include the dysregulation of immuno-inflammation and the loss of hepatocyte function, which leads to oxidative stress and endoplasmic reticulum stress [5,6]. At present, there are currently no effective treatments available for controlling organ injuries caused by THS [1]. Therefore, discovering drugs that can attenuate liver injury induced by THS is imperative.

Celastrol (Cel) derived from *Tripterygium wilfordii* is a natural compound with diverse bioactivities, exhibiting the potential to treat metabolic diseases and systemic inflammation [7]. In addition, Cel holds promise in protecting against chemicals that induce liver injury and cholestatic liver injury [8,9]. According to previous research, Cel has a protective effect on acute liver injury induced by

lipopolysaccharide by reducing oxidative stress, apoptosis and inflammation [10]. Given this particular conducive effect, Cel may have therapeutic potential in THS-induced live injury, although findings on the efficacy of Cel in this disease remain scarce.

It has been reported that Cel has a protective effect on hepatic steatosis by activating heat shock transcription factor 1 (*HSF1*). HSF1 plays a critical role in preventing inflammation and immune diseases [11,12], and negatively regulates the promoter of high mobility group box 1 (*HMGB1*) [13]. HMGB1 was a vital mediator of various pathological conditions, such as immune diseases, metabolic disorders and inflammation [14,15]. Moreover, HMGB1 is involved in immune pathogenesis by activating the toll-like receptor 9 (*TLR9*)/myeloid differentiation factor 88 (*MyD88*) pathway [16], which has been reported to promote inflammation and immune diseases [17,18]. A prior study has also demonstrated that ischemia-reperfusion injury and inflammation of the liver can be suppressed by inhibiting TLR9 and HMGB1 [19]. Presently, there are few studies revealing the effect of TLR9 on THS-induced liver injury. Based on these previous findings, we hypothesized that Cel regulates *HSF1* to inhibit the *TLR9*/*MyD88* pathway, thereby relieving liver injury induced by THS.

In this study, we aimed to explore the mechanism behind how Cel alleviates liver injury induced by THS in animal models.

Materials and Methods

Animal Experiment

Sixty Sprague–Dawley rats (8 weeks old, 250–280 g, male) obtained from Hangzhou Medical College (Hangzhou, China), were given free access to water and food and kept in a 12-hour light-dark cycle room set at 25 °C and 47% humidity. All experimental procedures involving animals were executed under the approval of the Ethics Committee of Zhejiang Baiyue Biotech Co., Ltd. for Experimental Animals Welfare (No. ZJBYLA-IACUC-20231120) and were implemented according to the guidelines of the China Council on Animal Care.

Establishment of the THS Model

THS model of rats was established according to previous research [20]. The rats were anesthetized by inhalation with 2% isoflurane (1349003, Sigma-Aldrich, St. Louis, MO, USA) during the operation with anesthesia machine (ABS-4, YUYAN, INSTRUMENTS, Shanghai, China). Rats were placed in the supine position on a table kept at a constant temperature of 37 °C. Clamp forceps were utilized to induce transverse fractures of the tibia and left lower limb femur of the rats. The abdominal midline was incised at a length of 5 cm, and the muscle layer was separated by an incision (until the abdominal organs were visible) and covered with saline-impregnated wet gauze. Then the neck down the trachea midline was incised to separate the blunt neck muscles and left carotid artery. The distal carotid artery and four proximal arteries were ligated and clamped by thread and clamps, respectively. Next, a small artery was cut open using a pair of surgical scissors and connected to a physiological monitor (PL2604, ADinstruments, Colorado Springs, CO, USA) by epidural anesthesia tube for continuous monitoring of mean arterial pressure (MAP), blood pressure, respiratory frequency, and heart rate. Afterwards, the femoral vein was separated by cutting the skin of the right lower limb, and an intravenous indwelling needle connected with the syringe was inserted into the vein. Then bloodletting from the femoral vein was performed to reduce the MAP to 30 mmHg, and the MAP was maintained between 30 and 40 mmHg for 90 min. The discharged blood, added with twice the volume of infusion solution, was infused back to the rats at a uniform rate for 30 min. Finally, a suture of the abdomen was performed after the needle was dislodged. For sham operations, the same surgery was performed on the rats, except that forceps clipping, bloodletting and fluid infusion were not conducted. After the modeling, one rat was found dead in the THS group and THS + Cel-0.5 group. The overall success rate of modeling was 96%; the success rate was calculated using the following formula:

$$\text{Success rate (\%)} = \text{Number of successful models} / \text{Total number of models} \times 100$$

Treatment and Grouping

The rats received an intraperitoneal injection of Cel (HY-13067, MedChemExpress, Princeton, NJ, USA) on the 7th day after the establishment of THS [10,21]. Cel was dissolved in a vehicle, which consisted of physiological saline (0.9% NaCl, 450006, Sigma-Aldrich, St. Louis, MO, USA) mixed with 1% dimethyl sulfoxide (34943, Sigma-Aldrich, St. Louis, MO, USA). The rats were divided into two parts. In the first part, 30 rats were divided into the sham, THS, THS + Cel-0.5, THS + Cel-1, and THS + Cel-1.5 groups (n = 6 per group). The rats in the sham group underwent sham operations; the rats in the THS, THS + Cel-0.5, THS + Cel-1, and THS + Cel-1.5 groups were subjected to all operation procedures mentioned above; additionally, the rats in the THS + Cel-0.5, THS + Cel-1, and THS + Cel-1.5 groups were intraperitoneally injected with 0.5, 1, and 1.5 mg/kg of Cel, respectively. In the second part, 30 rats were divided into the THS + Cel, THS + Cel + small interfering RNA (siRNA) negative control (siNC), THS + Cel + siRNA targeting heat shock transcription factor 1 (*siHSF1*), THS + Cel + *siHSF1* + siNC, and THS + Cel + *siHSF1* + siRNA targeting toll-like receptor 9 (*siTLR9*) (n = 6 per group). The rats in the THS + Cel group were subjected to all surgical operation procedures and injected intraperitoneally with 1.5 mg/kg of Cel; as for the latter four groups, 72 hours before the same surgery and injection, the rats were injected via the tail vein with lentivirus-

mediated siNC (psPAX2 + pMD2.G + pLVX-EGFP-IRES-puro encoded with siNC), *siHSF1* (psPAX2 + pMD2.G + pLVX-EGFP-IRES-puro encoded with *siHSF1*), *siHSF1* + siNC (psPAX2 + pMD2.G + pLVX-EGFP-IRES-puro encoded with *siHSF1*+ pLVX-EGFP-IRES-puro encoded with siNC), and *siHSF1* + *siTLR9* (psPAX2 + pMD2.G + pLVX-EGFP-IRES-puro encoded with *siHSF1* + pLVX-EGFP-IRES-puro encoded with *siTLR9*), respectively [22]. psPAX2, pMD2.G and pLVX-EGFP-IRES-puro were purchased from Addgene (12260, 12259, 128652, Watertown, MA, USA). siNC, *siHSF1* and *siTLR9* were obtained from Santa Cruz Biotechnology (sc-44230, sc-35612A, sc-40271B, Santa Cruz, CA, USA).

Transfection and Infection

pLVX-EGFP-IRES-puro was encoded with siNC, *siHSF1* (5′-CCGGCAGGAGCAGCTCCTTGAGATTCAAGAGATCTCAAGGAGCTGCTCCTGTTTTTG-3′) and *siTLR9* (5′-UGGACUGCAACUGGCUGUUCCUGAA-3′), respectively. HEK-293T cells were acquired from AnWei Biotechnology (AW-CELLS-H0004, Shanghai, China). The HEK-293T cells were maintained in Dulbecco's Modified Eagle Medium (DMEM, 11965092, Gibco, Grand Island, NY, USA) supplemented with 10% fetal bovine serum (FBS; A5669701, Gibco), 1% non-essential amino acid (NEAA; 11140050, Gibco) and 1% penicillin and streptomycin (P/S; 15070063, Gibco). The HEK-293T cells were cultured at 37 °C and 5% CO_2. The cells were proved to be mycoplasma-free and were authenticated by short tandem repeat (STR) profiling.

Afterwards, in order to acquire the lentivirus-mediated siNC/*siHSF1*/*siTLR9*, the HEK-293T cells (5×10^6 cells/dish) were inoculated into 10 cm culture dishes. The culture medium was replaced with a fresh medium, and the cells were transfected upon reaching a cell confluence of 80%. Opti-MEM™ reduced serum medium and Lipofectamine™ 3000 transfection reagent were acquired from Thermo Fisher Scientific (11058021, L3000001, Waltham, MA, USA). According to the manufacturer's protocol, solutions A and B were prepared: solution A encompasses 37.5 µL Lipofectamine™ 3000 mixed with 625 µL reduced serum medium; solution B contains 12 µg pLVX-EGFP-IRES-puro encoded with siNC/*siHSF1*/*siTLR9*, 9 µg psPAX2, 3 µg pMD2.G, 625 µL reduced serum medium, and 25 µL P3000™. Then, 625 µL of solution A and 625 µL of solution B were combined, gently mixed and incubated at room temperature for 15 min. The mixture was slowly added to the cells. After overnight incubation, the culture medium was replaced with a fresh medium. Then the cellular supernatant of each dish was collected, and fresh medium was supplemented after 48 h. Again, the cellular supernatant of each dish was harvested after 24 h. Lentivirus-mediated plasmids (1×10^8 TU/mL) were obtained after filtration, concentration and purification of the cellular supernatant, and stored at –80 °C. Then, 72 hours before the treatment mentioned above, the rats from the THS + Cel + siNC, THS + Cel + *siHSF1*, THS + Cel + *siHSF1* + siNC, and THS + Cel + *siHSF1* + *siTLR9* groups were injected via the tail vein with lentivirus-mediated 0.1 mL siNC, 0.1 mL *siHSF1*, 0.1 mL *siHSF1* + 0.1 mL siNC, and 0.1 mL *siHSF1* + 0.1 mL *siTLR9*, respectively.

Each rat received an intraperitoneal injection of 1% sodium pentobarbital (45 mg/kg body weight, P3761, Sigma, MO, USA) 24 hours after having been given the treatments mentioned above. The liver tissue of rats in each group was collected. Meanwhile, whole blood was collected from the inferior vena cava. The whole blood collected was incubated at room temperature for 2 hours and centrifuged at 3000 rpm for 15 min to obtain the serum. The rats were then euthanized with an overdose of sodium pentobarbital (200 mg/kg, Intraperitoneal injection, P3761, Sigma-Aldrich, St. Louis, Missouri, USA).

Hematoxylin-Eosin Staining

Paraffin sections of rat liver tissue in each group were prepared by means of paraffin embedding (A601888; Sangon Biotech, Shanghai, China) and using a tissue slicer (RM2125 RTS, Leica, Hessian, Germany). Tissue slices were immersed in xylene (X112050, Aladdin, Shanghai, China) twice for 5 min. Afterwards, tissue slices were rinsed with a series of graded ethanol (100% for 5 min, 95% for 3 min, 90% for 3 min, 80% for 3 min, 70% for 3 min). Hematoxylin-eosin (HE) staining assay kit (C0105S; Beyotime, Shanghai, China) was utilized to highlight the morphology of rat liver tissue. Each sample was incubated with a hematoxylin staining solution for 8 min and then washed with water for 10 min. Next, each sample was immersed in an eosin staining solution for 1 min and dehydrated after washing with water. Each sample was incubated with xylene for 5 min and sealed with neutral gum (G8590; Solarbio, Beijing, China). Finally, staining results were observed under a light microscope (magnification ×100; LV150, Nikon Inc., Tokyo, Japan).

Enzyme-Linked Immunosorbent Assay (ELISA)

Rat ELISA kits (ab234579, ab263883, ab236712, ab255730, Abcam, Cambridge, UK; NBP2-69939, Novus Biologicals, Littleton, CO, USA) were applied to detect the serum levels of alanine aminotransferase (ALT), aspartate aminotransferase (AST), tumor necrosis factor-alpha (TNF-α), interleukin-1 beta (IL-1β), and total bilirubin (TB) for rats in each group. The serum was diluted 100 times with diluent. For TB, 100 µL capture antibody solution was dispensed into the wells. After overnight incubation at 4 °C, each well was washed with wash buffer twice. Each well was added with 300 µL reagent diluent incubated at room temperature for 60 min and washed two times. Then each well was added with 100 µL diluted serum and incubated, along with corresponding standards, for 2 hours at room temperature. After incubation, the wells were washed

Table 1. The primer sequences of related genes.

Gene	Forward primer (5′-3′)	Reverse primer (5′-3′)
Bcl2 (Rat)	GGGGATGACTTCTCTCGTCG	GACATCTCCCTGTTGACGCT
Bax (Rat)	CAACATGGAGCTGCAGAGGA	GGGGTCCCGAAGTAGGAAAG
β-actin (Rat)	CCGCGAGTACAACCTTCTTG	CAGTTGGTGACAATGCCGTG

Bcl2, B-cell lymphoma 2; *Bax*, B-cell lymphoma 2 associated X protein.

twice. Next, each well was added with 100 µL detection antibody solution incubated for 2 hours at room temperature and washed with wash buffer. Afterwards, each well was dispensed with 100 µL substrate solution and incubated at room temperature for 20 min in the dark and washed twice. Finally, each well was added with 50 µL stop solution.

For ALT, AST, TNF-α, and IL-1β, 50 µL diluted serum and corresponding standards were added to the wells coated with respective antibodies, and then 50 µL respective enzyme-linked antibody solution was added. After incubation for 1 hour at room temperature, each well was washed with 350 µL wash buffer three times. Next, each well was added with 100 µL TMB solution and incubated at room temperature in the dark for 10 min. Eventually, the reaction in each well was stopped by adding 100 µL stop solution, and the optical density of each well was measured at 450 nm using a microplate reader (SpectraMax ABS plus, Molecular Devices, Sunnyvale, CA, USA). The experiments were repeated three times.

Quantitative Real-Time Polymerase Chain Reaction

Quantitative real-time polymerase chain reaction (qRT-PCR) was implemented to estimate the expression levels of B-cell lymphoma 2 (*Bcl2*) and B-cell lymphoma 2 associated X protein (*Bax*) in rat liver tissue. Total RNA was isolated using an RNA Extraction Kit (R0017S, Beyotime). Furthermore, NanoDrop™ One (701-058112, Thermo Fisher Scientific, Waltham, MA, USA) was utilized to detect the concentration and quality of total RNA. Next, cDNA was synthesized from total RNA using an RT Reagent Kit (RR092S, Takara, Osaka, Japan). Then reaction solution containing cDNA and ingredients from qRT-PCR Reagent Kit (RR820Q, Takara, Osaka, Japan) was prepared and subjected to PCR amplification for 40 cycles (95 °C denaturation for 5 sec, 60 °C annealing for 30 sec). StepOnePlus Real-time PCR System (4376598, Thermo Fisher Scientific) was utilized to perform qRT-PCR. All samples were prepared in triplicate and all experiments were repeated three times. The data collected were analyzed using the $2^{-\Delta\Delta Ct}$ method [23], with β-actin being the internal reference. The primers (Table 1) used in this experiment were generated by GenScript (Piscataway, NJ, USA).

Biochemical Analysis

Indicators of oxidative stress in rat liver tissue were measured by reactive oxygen species (ROS) Assay Kit (BB-470516, BestBio, Shanghai, China), Superoxide Dismutase (SOD) Assay Kit (S0101S, Beyotime, Shanghai, China), Glutathione (GSH) Assay Kit (S0053, Beyotime, Shanghai, China), and Malondialdehyde (MDA) Assay Kit (S0131S, Beyotime, Shanghai, China).

For the detection of ROS, frozen slices of rat liver tissue each measuring 10–20 µm in thickness were cut using a frozen slicer (CM1860, Leica, Hessian, Germany). Then each slice was immersed in 200 µL wash buffer for 5 min. After the wash buffer was removed, each slice was immersed in 200 µL staining solution and incubated in the dark at 37 °C for 60 min. Next, each slice was washed thrice and then covered with a coverslip. Each slice was observed under a fluorescence microscope (magnification ×400; IX70, Olympus, Tokyo, Japan).

For the detection of SOD, 10 mg of rat liver tissue was homogenized in 100 µL of SOD sample preparation solution using a dispersing instrument (0020013564, IKA, Staufen, Germany) at 4 °C. Then each homogenate sample was centrifuged at 12,000 ×g for 5 min, and the supernatant of each sample was aspirated and diluted 10 times by SOD detection buffer. Afterwards, 20 µL of each sample/standard, 160 µL of working solution, and 20 µL of reaction start-up working solution were added to the 96-well plates. After 30 min of incubation at 37 °C, the absorbance at 450 nm of each sample was measured by a microplate reader (SpectraMax ABS plus, Molecular Devices, San Jose, CA, USA).

For the detection of GSH, 10 mg of rat liver tissue was homogenized in 100 µL of protein removal reagent. After incubation of each homogenate sample for 10 min at 4 °C and centrifugation for 10 min at 10,000 ×g, the supernatant of each sample was aspirated and diluted 5 times with protein removal reagent. Next, a portion of each sample was diluted with GSH removal buffer at a ratio of 100 µL of each sample to 20 µL of GSH removal buffer. After mixing, each sample was added to the GSH removal solution at a ratio of 100 µL of each sample to 4 µL of GSH removal solution; the mixture was then incubated at 25 °C for 60 min. Meanwhile, 10 µL of each sample/standard and 150 µL of working solution were added to the 96-well plates. After 5 min of incubation at room temperature, 50 µL of nicotinamide adenine dinucleotide phosphate (NADPH, 0.5 mg/mL) was added to each well. The absorbance was measured at 450 nm.

For the detection of MDA, 10% (w/v) homogenate of each sample was obtained by homogenizing rat liver

Table 2. List of antibodies used in this study.

Name	Catalog	Molecular weight	Dilution	Manufacturer
HSF1	ab61382	57 kDa	1/1000	Abcam, Cambridge, UK
TLR9	ab187148	116 kDa	1/1000	Abcam, Cambridge, UK
MyD88	ab133739	33 kDa	1/1000	Abcam, Cambridge, UK
β-actin	ab8226	42 kDa	1/1000	Abcam, Cambridge, UK
Goat anti-rabbit	ab97051	—	1/10,000	Abcam, Cambridge, UK
Goat anti-mouse	ab96879	—	1/10,000	Abcam, Cambridge, UK
Goat anti-rat	ab97057	—	1/10,000	Abcam, Cambridge, UK

HSF1, heat shock transcription factor 1; TLR9, toll-like receptor 9; MyD88, myeloid differentiation factor 88.

tissue in phosphate-buffered saline (PBS; 10010023, Gibco, Grand Island, NY, USA). Then 0.1 mL of homogenate/standard mixed with 0.2 mL of MDA assay solution was incubated at 100 °C for 15 min. After the mixture was cooled to room temperature and centrifuged at 1000 $\times$g for 10 min, 200 µL of each sample's supernatant was aspirated and dispensed into the 96-well plates. The absorbance was measured at 532 nm. All experiments were conducted three times.

Western Blotting

Total proteins were isolated from rat liver tissue using a total protein extraction kit (R0018S, Beyotime) to detect the protein expression levels of HSF1, TLR9 and MyD88 by means of Western blotting. Bicinchoninic Acid (BCA) Protein Assay kit (ZJ101, Epizyme, Shanghai, China) was utilized to measure the concentration of total proteins. Denaturation of total proteins was performed by incubating the samples in boiling water for 5 min. Sodium dodecyl sulfate–polyacrylamide gel electrophoresis (SDS-PAGE) was conducted to separate proteins, which were then transferred to Polyvinylidene difluoride (PVDF) membranes (IPVH00010, Millipore, Bedford, MA, USA). Each membrane was blocked using a blocking buffer (P0023B, Beyotime, Shanghai, China) at room temperature for 1 h. Next, each membrane was soaked with primary antibodies targeting HSF1, TLR9, MyD88 and β-actin, respectively, at 4 °C overnight, and then with secondary antibodies, including goat anti-mouse, goat anti-rabbit and goat anti-rat antibodies, at 25 °C for 1 h. All antibodies utilized are listed in Table 2. β-actin was treated as the internal reference. Protein blots were developed using BeyoECL Moon (P0018FS, Beyotime, Shanghai, China). The protein blots were photographed by the iBright CL1500 imaging system (A44240, Thermo Fisher Scientific, Waltham, MA, USA). Finally, ImageJ 1.8.0 software (National Institutes of Health, Bethesda, MD, USA) was used to quantify the protein expression. The experiments were repeated at least three times.

Statistical Analyses

GraphPad Prism 8.0 (GraphPad Software Inc., San Diego, CA, USA) was used for statistical analyses. All measurement data are expressed as mean $\pm$ standard deviation. Multi-group comparisons were analyzed using one-way analysis of variance (ANOVA) coupled with the Tukey test for post-hoc analysis. Differences were considered statistically significant at $p < 0.05$.

Results

Cel Attenuated THS-Induced Liver Injury

Histological observation of HE-stained rat liver tissue revealed that compared with the sham group, liver lobules in the THS group were congested and structurally incomplete, displaying structural aberrations of hepatocytes, swelling of hepatocytes, and infiltration of inflammatory cells (Fig. 1A). However, pathological alterations of rat liver tissue were progressively attenuated with the increasing concentrations of Cel administered (Fig. 1A). In addition, compared with the sham group, the levels of ALT, AST, TB, TNF-α, and IL-1β in the THS group were significantly increased (Fig. 1B–F, $p < 0.001$), but the levels of these five indicators in the THS + Cel-0.5, THS + Cel-1, and THS + Cel-1.5 groups were decreased in contrast to the THS group (Fig. 1B–F, $p < 0.001$). Furthermore, the THS group exhibited lower Bcl2 and higher Bax expression levels than the sham group (Fig. 1G,H, $p < 0.001$). The Cel administration negated the THS-induced changes of these two indicators by raising the expression level of Bcl2 and reducing the expression level of Bax in a dose-dependent manner (Fig. 1G,H, $p < 0.001$).

The abundance of ROS was also increased in the THS group compared to the sham group, but gradually diminished with the increasing concentrations of Cel (Fig. 2A). Additionally, compared with the sham group, the THS group demonstrated a higher level of oxidative stress, marked by elevated MDA content as well as decreased GSH concentration and SOD activity (Fig. 2B–D, $p < 0.001$). However, oxidative stress could be counteracted by the administration of Cel by improving the profile of these indicators (Fig. 2B–D, $p < 0.001$).

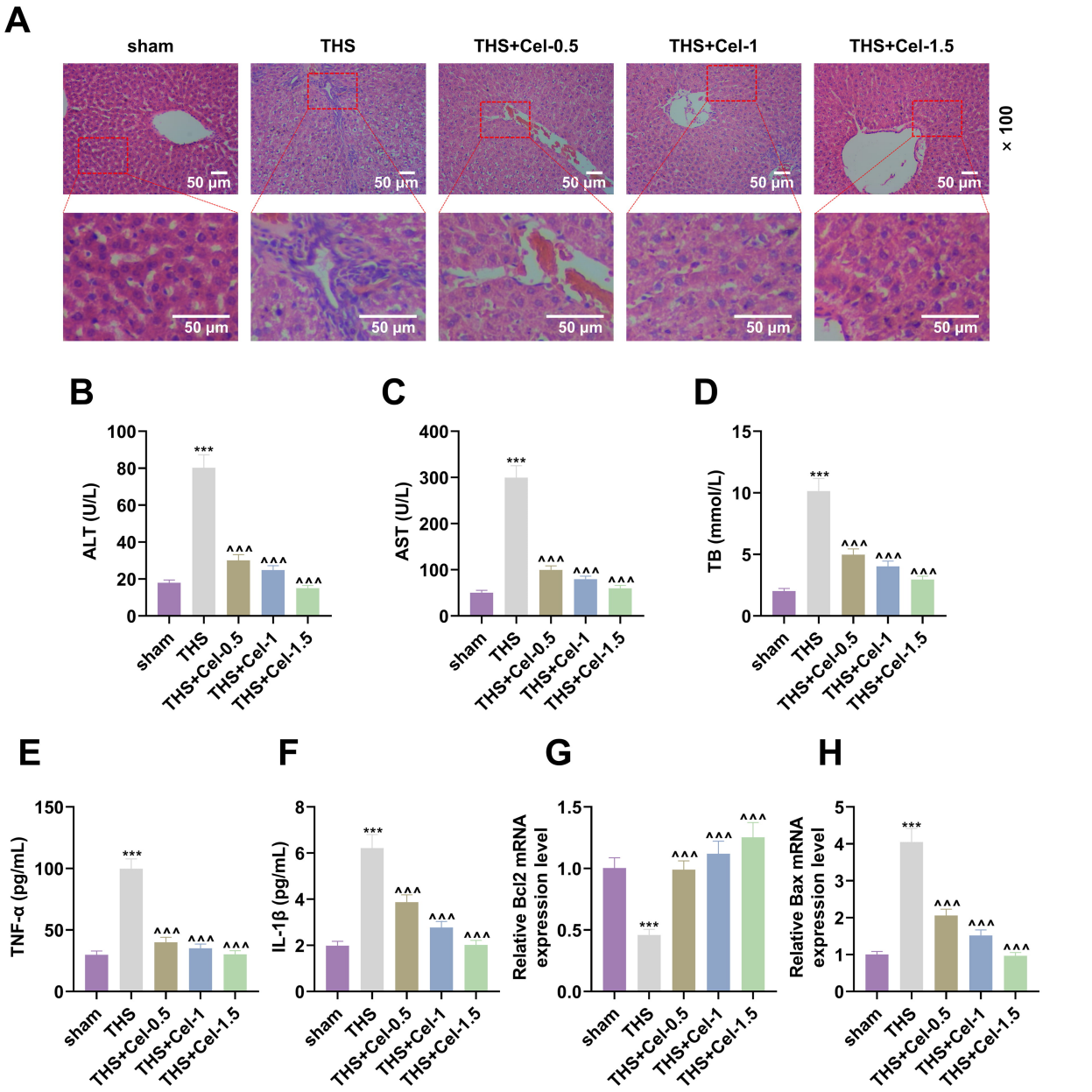

Fig. 1. Effects of Cel on liver injury, inflammation and apoptosis. (A) Histopathological alterations of rat liver tissue in each group as observed by HE staining. Scale bar: 50 μm; magnification: ×100. (B–D) Serum levels of liver injury indicators (ALT, AST, TB) in each group as determined by ELISA. (E,F) Serum levels of inflammation indicators (TNF-α, IL-1β) in each group as measured by ELISA. (G,H) Expression levels of *Bcl2* and *Bax* in rat liver tissue of each group as detected by qRT-PCR, with β-actin being the internal reference. ***$p < 0.001$ vs. sham group; $^{\wedge\wedge\wedge}p < 0.001$ vs. THS group. Abbreviations: Cel, celastrol; THS, traumatic hemorrhagic shock; HE, hematoxylin-eosin; ALT, alanine aminotransferase; AST, aspartate aminotransferase; TB, total bilirubin; ELISA, enzyme-linked immunosorbent Assay; TNF-α, tumor necrosis factor-alpha; IL-1β, interleukin-1 beta; *Bcl2*, B-cell lymphoma 2; *Bax*, B-cell lymphoma 2 associated X protein; qRT-PCR, quantitative real-time polymerase chain reaction.

In the THS group, the expression levels of TLR9 and MyD88 were obviously increased and HSF1 displayed a significantly lower expression level, as compared to the sham group (Fig. 3, $p < 0.001$). However, such alterations of these proteins could be reversed by Cel administration (Fig. 3, $p < 0.001$).

Cel Attenuated THS-Induced Liver Injury by Regulating the TLR9 Pathway via HSF1

To further investigate whether Cel relieved THS-induced liver injury through the *TLR9* pathway, lentivirus-mediated siNC, *siHSF1* and *siTLR9* were injected into rats. According to the Western blot results, the expression levels

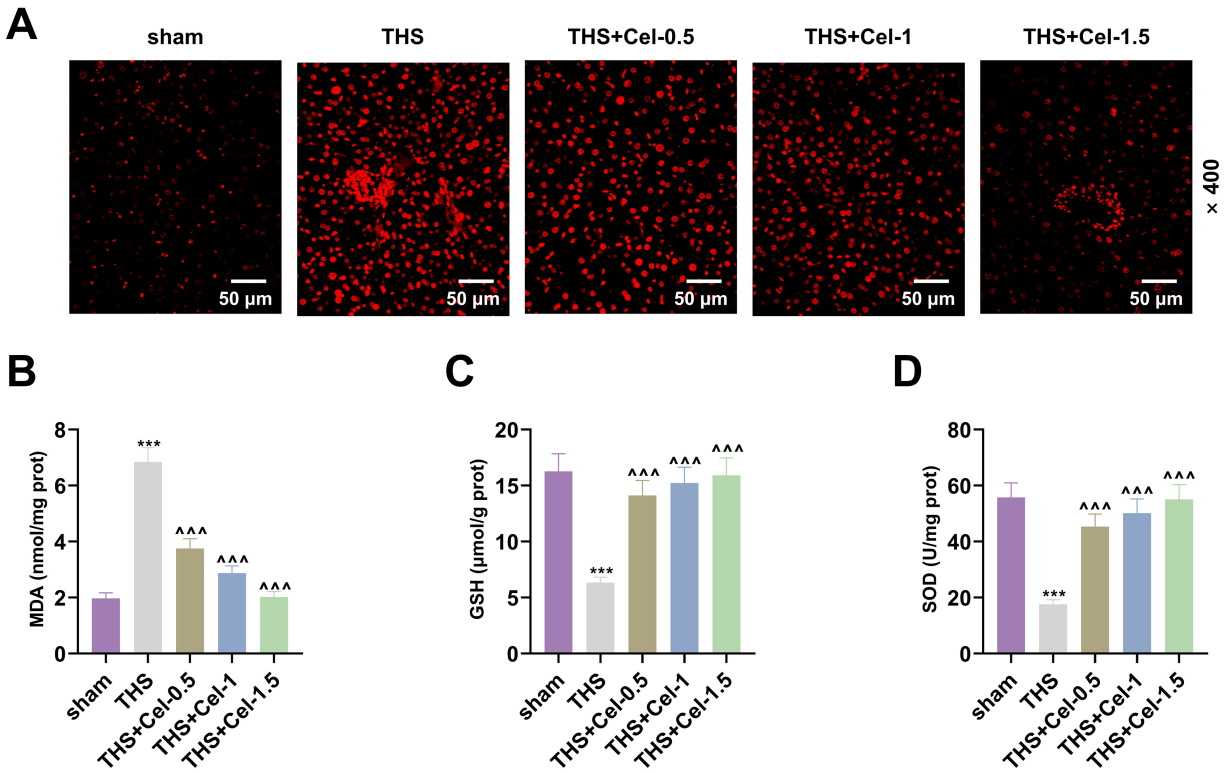

Fig. 2. Effects of Cel on the indicators of oxidative stress in rat liver tissue. (A) Abundance of ROS in rat liver tissue of each group as detected using fluorescent probes. Scale bar: 50 μm; magnification: ×400. (B–D) Levels of oxidative stress indicators (MDA, GSH, SOD) in rat liver tissue of each group. ***$p < 0.001$ vs. sham group; ^^^$p < 0.001$ vs. THS group. Abbreviations: Cel, celastrol; ROS, reactive oxygen species; MDA, malondialdehyde; GSH, glutathione; SOD, superoxide dismutase; THS, traumatic hemorrhagic shock.

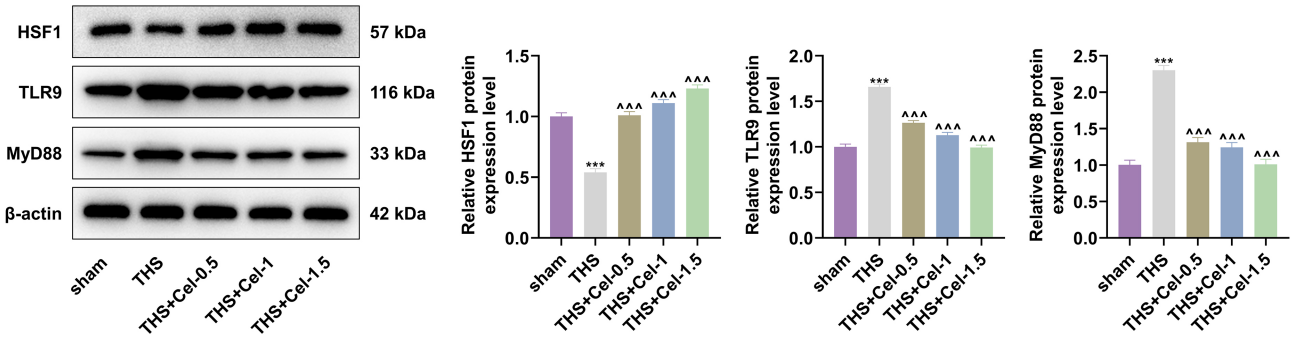

Fig. 3. Effects of Cel on the protein expression levels of HSF1, TLR9 and MyD88 in rat liver tissue. Western blot was utilized to determine the protein expression levels of HSF1, TLR9 and MyD88 in rat liver tissue of each group. β-actin was employed as the internal reference. ***$p < 0.001$ vs. sham group; ^^^$p < 0.001$ vs. THS group. Abbreviations: Cel, celastrol; HSF1, heat shock transcription factor 1; TLR9, toll-like receptor 9; MyD88, myeloid differentiation factor 88; THS, traumatic hemorrhagic shock.

of TLR9 and MyD88 in the THS + Cel + *siHSF1* group were significantly escalated compared to the THS + Cel + siNC group (Fig. 4, $p < 0.001$). TLR9 and MyD88 in the THS + Cel + *siHSF1* + *siTLR9* group exhibited remarkably reduced expression levels relative to the THS + Cel + *siHSF1* + siNC group (Fig. 4, $p < 0.001$).

According to the HE staining results, silencing of *HSF1* in the THS + Cel + *siHSF1* group exacerbated pathological damage of rat liver tissue as compared to the THS + Cel + siNC group (Fig. 5A), and silencing of *TLR9* alleviated the pathological damage of rat liver tissue caused by silencing of *HSF1* (Fig. 5A). In addition, compared to the THS + Cel + siNC group, the THS + Cel + *siHSF1* group exhibited significantly increased ALT, AST, TB, TNF-α and IL-1β levels (Fig. 5B–F, $p < 0.001$), which could be offset by the silencing of *TLR9* (Fig. 5B–F, $p < 0.001$). Furthermore, the gene expression results demonstrated that *HSF1* silencing in the THS + Cel + *siHSF1* group downregulated

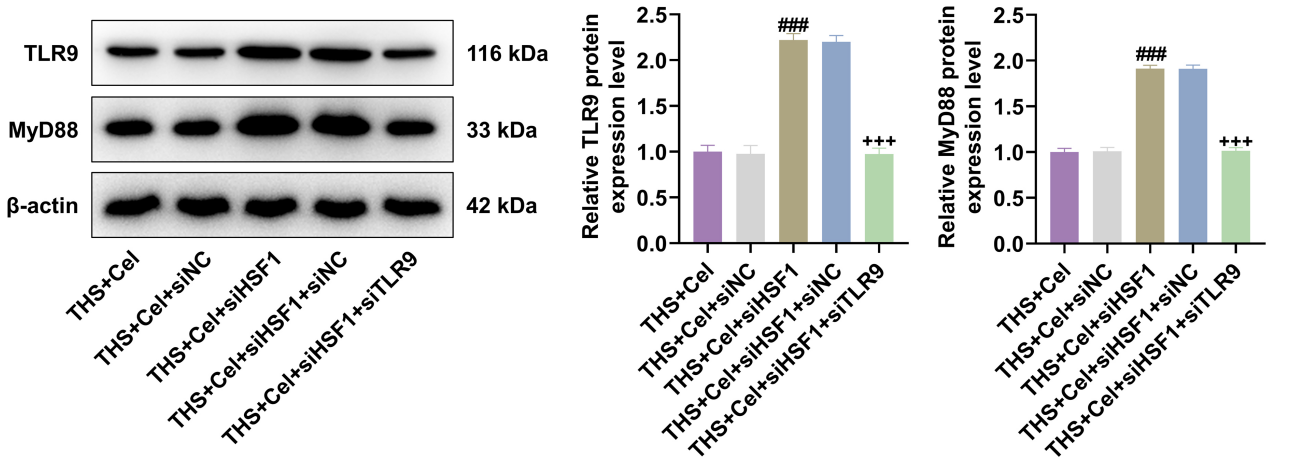

Fig. 4. TLR9 silencing reversed the increased expression levels of TLR9 and MyD88 caused by HSF1 silencing. The protein expression levels of TLR9 and MyD88 in rat liver tissue of each group were determined by means of Western blotting. β-actin was employed as the internal reference. $^{###}p < 0.001$ vs. THS + Cel + siNC group; $^{+++}p < 0.001$ vs. THS + Cel + *siHSF1* + siNC group. Abbreviations: TLR9, toll-like receptor 9; MyD88, myeloid differentiation factor 88; HSF1, heat shock transcription factor 1; THS, traumatic hemorrhagic shock; Cel, celastrol; siNC, small interfering RNA negative control; *siHSF1*, siRNA targeting heat shock transcription factor 1.

Bcl2 expression and upregulated *Bax* expression, relative to the THS + Cel + siNC group (Fig. 5G,H, $p < 0.001$), but the effects of *HSF1* silencing on the expression levels of *Bcl2* and *Bax* could be reversed by silencing *TLR9* (Fig. 5G,H, $p < 0.001$).

Cel Attenuated THS-Induced Oxidative Stress by Regulating the TLR9 Pathway via HSF1

HSF1 silencing elevated ROS abundance, whereas silencing of TLR9 led to the reduced abundance of ROS (Fig. 6A). Moreover, compared to the THS + Cel + siNC group, the THS + Cel + *siHSF1* group demonstrated that silencing of *HSF1* led to significantly increased MDA content as well as decreased GSH concentration and SOD activity (Fig. 6B–D, $p < 0.001$). Our results further showed that silencing of *TLR9* reversed the changes in these oxidative stress indicators due to HSF1 silencing (Fig. 6B–D, $p < 0.001$).

Discussion

THS is defined as hypovolemic shock triggered by trauma [24,25]. Organ failures represent a complication of THS due to decreased circulating blood volume [26]. The liver is particularly more susceptible to the injury consequent to THS due to the organ's critical role in homeostasis and metabolism [27]. In addition, the degree of liver injury is strongly associated with mortality [26]. As described in previous studies, Sprague–Dawley rats are commonly applied to establish an animal model of THS [28,29]. The THS rats manifest several distinctive hallmarks, such as augmented levels of serum inflammatory markers, as well as pathological alterations, apoptosis and oxidative stress in rat liver tissue [22,30,31], all of which were recapitulated in the current study.

It has been discovered that Cel boasts a protective effect on liver injury and anti-inflammatory properties against liver fibrosis [32,33]. A growing line of evidence also indicates that Cel can attenuate liver injury, inflammation, oxidative stress and apoptosis in rats [34–37]. Another study indicated that Cel holds the potential for suppressing hepatic ischemia-reperfusion injury [38]. Consistent with the studies mentioned above, our research demonstrated that Cel can alleviate liver injury, inflammation, apoptosis and oxidative stress in THS rats. To the best of our knowledge, treating THS with Cel has not been widely investigated, presenting a new research direction to improve the existing therapies.

Furthermore, a recent study revealed that Cel activates HSF1 to reduce accumulated fats in cells [39]. It has also been shown that the activation of HSF1 ameliorates inflammatory liver injury and hepatic ischemia-reperfusion injury [40,41]. The present study revealed that Cel raised the expression level of HSF1 to attenuate THS-induced liver injury. Interestingly, our results also showed that Cel inhibits the TLR9/MyD88 expression. According to previous studies, TLR9 exacerbates liver injury and promotes inflammatory response [42,43], whereas MyD88 drives inflammatory response and the development of acute liver injury [44,45]. Moreover, our result showed that HSF1 silencing augmented TLR9/MyD88 expression. Several studies have discovered that HSF1 may play a vital role in Cel treatment of THS by regulating the TLR9/MyD88 pathway [13,16,46]. In the current study, the expression level

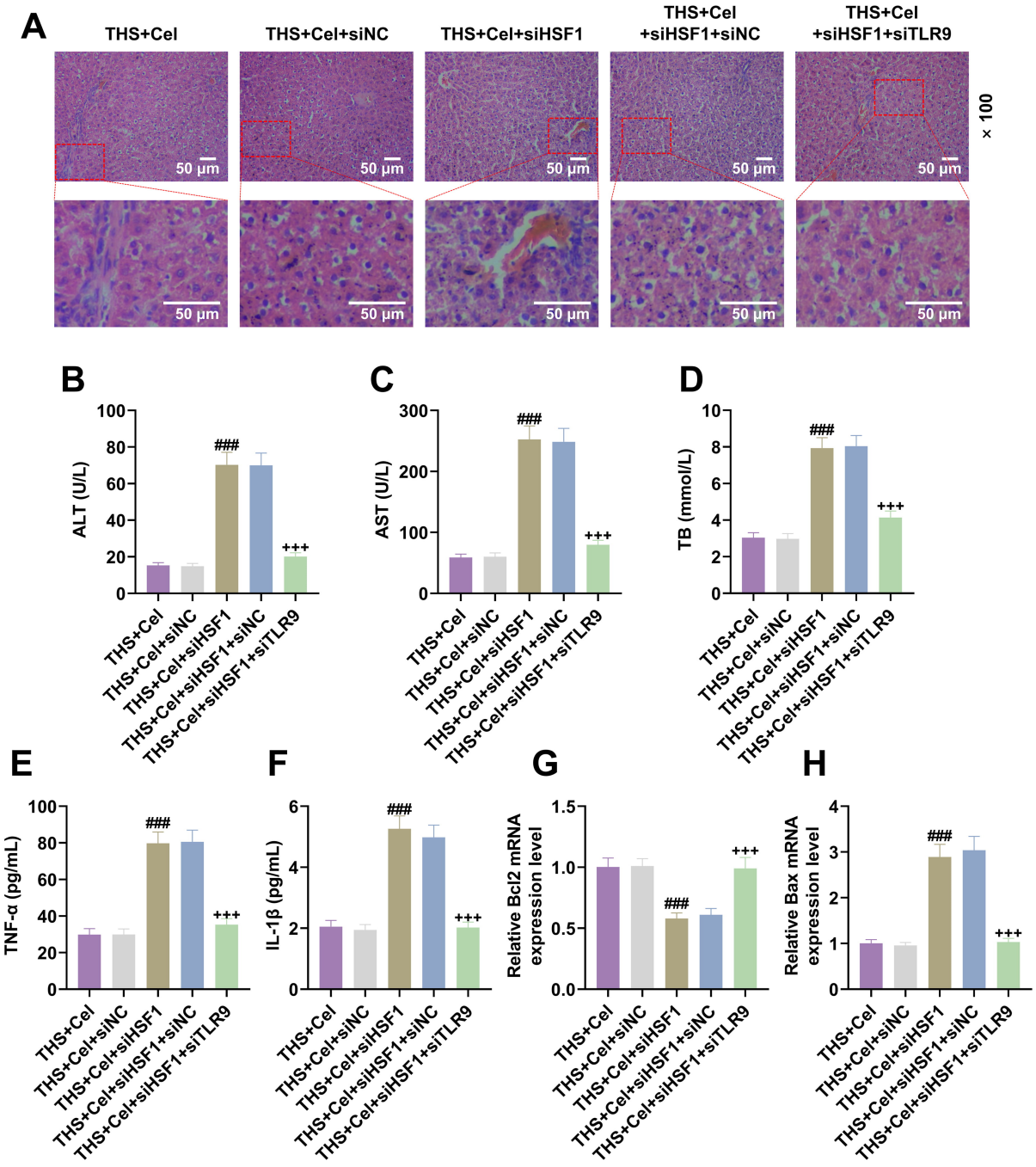

Fig. 5. TLR9 silencing reversed the effects of HSF1 silencing on liver injury, inflammation and apoptosis in rat serum and liver tissue. (A) Histopathological alterations of rat liver tissue in each group as highlighted through HE staining. Scale bar: 50 μm; magnification: ×100. (B–D) Serum levels of liver injury indicators (ALT, AST, TB) in each group as measured by ELISA. (E,F) Serum levels of inflammation indicators (TNF-α, IL-1β) in each group as determined by ELISA. (G,H) Expression levels of *Bcl2* and *Bax* in rat liver tissue of each group as estimated by qRT-PCR, with β-actin being employed as the internal reference. $^{\#\#\#}p < 0.001$ vs. THS + Cel + siNC group; $^{+++}p < 0.001$ vs. THS + Cel +*siHSF1* + siNC group. Abbreviations: TLR9, toll-like receptor 9; HSF1, heat shock transcription factor 1; HE, hematoxylin-eosin; ELISA, enzyme-linked immunosorbent assay; ALT, alanine aminotransferase; AST, aspartate aminotransferase; TB, total bilirubin; TNF-α, tumor necrosis factor-alpha; IL-1β, interleukin-1 beta; qRT-PCR, quantitative real-time polymerase chain reaction; *Bcl2*, B-cell lymphoma 2; *Bax*, B-cell lymphoma 2 associated X protein; THS, traumatic hemorrhagic shock; Cel, celastrol; siNC, small interfering RNA negative control.

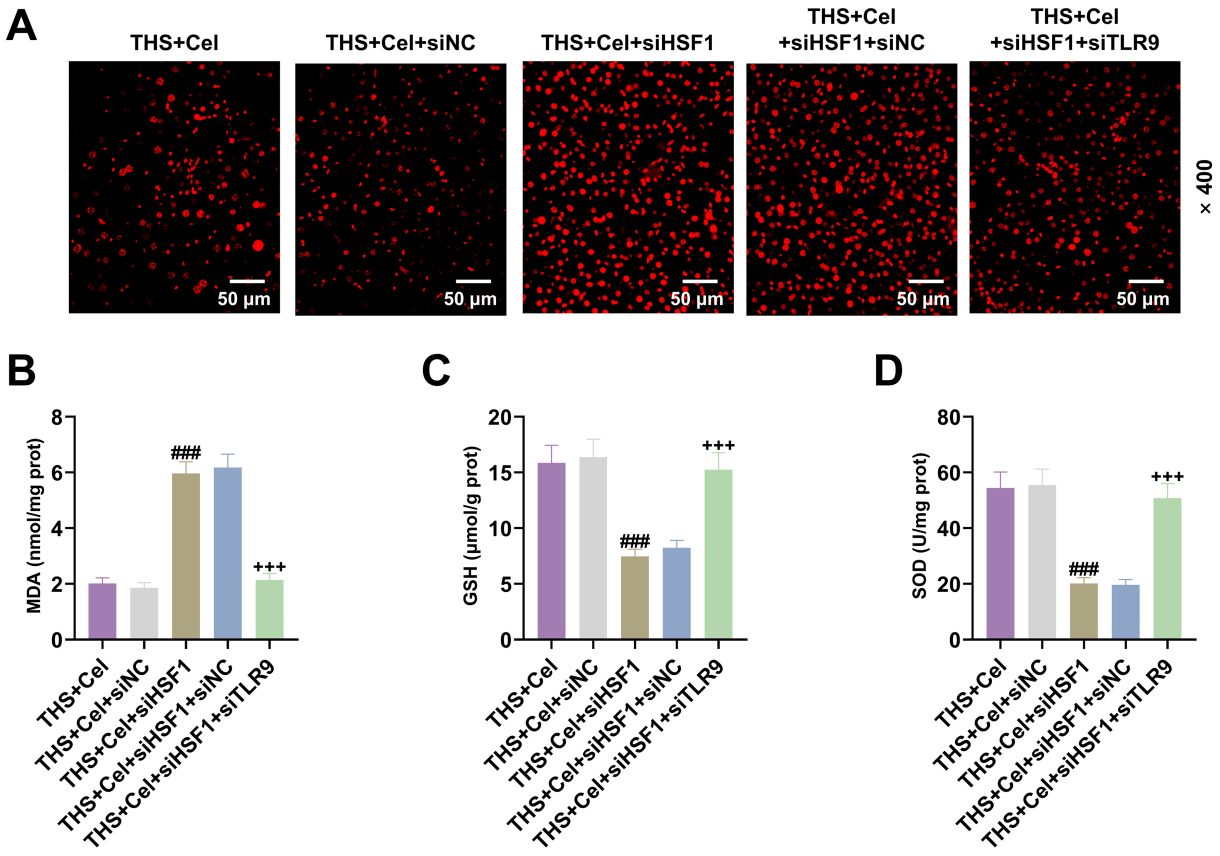

Fig. 6. TLR9 silencing reversed the effects of HSF1 silencing on the indicators of oxidative stress in rat liver tissue. (A) Abundance of ROS in rat liver tissue of each group as detected by fluorescent probes. Scale bar: 50 μm; magnification: ×400. (B–D) Levels of oxidative stress indicators (MDA, GSH, SOD) in rat liver tissue of each group. $^{###}p < 0.001$ vs. THS + Cel + siNC group; $^{+++}p < 0.001$ vs. THS + Cel +*siHSF1* + siNC group. Abbreviations: TLR9, toll-like receptor 9; HSF1, heat shock transcription factor 1; ROS, reactive oxygen species; MDA, malondialdehyde; GSH, glutathione; SOD, superoxide dismutase; THS, traumatic hemorrhagic shock; Cel, celastrol; siNC, small interfering RNA negative control.

of TLR9 was suppressed by Cel-induced HSF1 activation, thereby mitigating inflammation and liver injury.

Despite the preliminary findings connecting HSF1 with TLR9 presented in this paper, further studies are still warranted to explore how HSF1 and TLR9 are regulated. In this respect, a research direction has been foreshadowed by a number of previous studies, providing insight into how both HSF1 and TLR9 are regulated. A previous study showed that TLR9 regulates the expression of NF-κB via MyD88 [47]. It has been found that the TLR9/Myd88/NF-κB signaling pathway is strongly associated with the progression of ulcerative colitis [48]. On a separate note, another study found that heat stress stimulates NF-κB-mediated pro-apoptosis of IEC-6 cells by regulating the activation of HSF1 [49]. As demonstrated by these studies, central to the link between HSF1 and TLR9 is the inextricable involvement of the NF-kB signaling pathway, which is worthy of more in-depth experimental verification.

In summary, the molecular mechanism underlying the amelioration of THS-induced liver injury by Cel treatment involves the upregulation of the HSF1 expression to suppress the expression of TLR9 and MyD88. The therapeutic effect of Cel in THS-induced liver injury increases with the concentration of the administered Cel.

The current study is not without limitations. Firstly, the TLR9/MyD88 pathway was not investigated in-depth in this study; therefore; further experiments should be conducted to unravel the pathway with a focus on MyD88. In addition, the interactions of HMGB1 with HSF1 and TLR9/MyD88 were not mentioned in this study, warranting more in-depth investigations to elucidate the complete pathway behind the Cel treatment of THS-induced liver injury. To ensure successful clinical translation in the future, double-blind experiments are required to validate the efficacy of the Cel treatment in human patients with THS-induced liver injury.

Conclusions

This study delineates the molecular mechanism behind the alleviation of THS-induced liver injury by Cel

treatment, which involves the upregulation of HSF1 expression and the subsequent inhibition of TLR9 expression. Through this study, we discovered the beneficial effects of Cel in ameliorating THS-induced liver injury, providing fresh insights for advancing the treatment for this disease and further deciphering the underlying mechanism.

Availability of Data and Materials

The analyzed data sets generated during the study are available from the corresponding author upon reasonable request.

Author Contributions

JZ, XS designed the research study; YZ performed the research; YZ collected and analyzed the data. All authors have been involved in drafting the manuscript and all authors have been involved in revising it critically for important intellectual content. All authors have given the final approval of the version to be published. All authors have participated sufficiently in the work to take public responsibility for appropriate portions of the content and agreed to be accountable for all aspects of the work in ensuring that questions related to its accuracy or integrity.

Ethics Approval and Consent to Participate

All experimental operations on SD rats were executed under the approval of the Ethics Committee of Zhejiang Baiyue Biotech Co., Ltd. for Experimental Animals Welfare (No. ZJBYLA-IACUC-20231120), and were implemented according to the guidelines of the China Council on Animal Care.

Acknowledgment

Not applicable.

Funding

This research received no external funding.

Conflict of Interest

The authors declare no conflict of interest.

References

[1] Valade G, Libert N, Martinaud C, Vicaut E, Banzet S, Peltzer J. Therapeutic Potential of Mesenchymal Stromal Cell-Derived Extracellular Vesicles in the Prevention of Organ Injuries Induced by Traumatic Hemorrhagic Shock. Frontiers in Immunology. 2021; 12: 749659.

[2] Cannon JW. Hemorrhagic Shock. The New England Journal of Medicine. 2018; 378: 370–379.

[3] Taniguchi T, Fujimoto Y, Yawata H, Horiguchi M, An B, Takegami T, *et al*. Renal venous congestion following hemorrhagic shock due to traumatic liver injury. CEN Case Reports. 2021; 10: 178–183.

[4] Liu H, Xiao X, Sun C, Sun D, Li Y, Yang M. Systemic inflammation and multiple organ injury in traumatic hemorrhagic shock. Frontiers in Bioscience (Landmark Edition). 2015; 20: 927–933.

[5] Dufour-Gaume F, Frescaline N, Cardona V, Prat NJ. Danger signals in traumatic hemorrhagic shock and new lines for clinical applications. Frontiers in Physiology. 2023; 13: 999011.

[6] Li M, Xie F, Wang L, Zhu G, Qi LW, Jiang S. Celastrol: An Update on Its Hepatoprotective Properties and the Linked Molecular Mechanisms. Frontiers in Pharmacology. 2022; 13: 857956.

[7] Luo P, Zhang Q, Zhong TY, Chen JY, Zhang JZ, Tian Y, *et al*. Celastrol mitigates inflammation in sepsis by inhibiting the PKM2-dependent Warburg effect. Military Medical Research. 2022; 9: 22.

[8] Jannuzzi AT, Kara M, Alpertunga B. Celastrol ameliorates acetaminophen-induced oxidative stress and cytotoxicity in HepG2 cells. Human & Experimental Toxicology. 2018; 37: 742–751.

[9] Zhao Q, Tang P, Zhang T, Huang JF, Xiao XR, Zhu WF, *et al*. Celastrol ameliorates acute liver injury through modulation of PPARα. Biochemical Pharmacology. 2020; 178: 114058.

[10] Yang T, Zhao S, Sun N, Zhao Y, Wang H, Zhang Y, *et al*. Network pharmacology and in vivo studies reveal the pharmacological effects and molecular mechanisms of Celastrol against acute hepatic injury induced by LPS. International Immunopharmacology. 2023; 117: 109898.

[11] Yu L, Zhou B, Zhu Y, Li L, Zhong Y, Zhu L, *et al*. HSF1 promotes CD69$^+$ Treg differentiation to inhibit colitis progression. Theranostics. 2023; 13: 1892–1905.

[12] Janus P, Kuś P, Vydra N, Toma-Jonik A, Stokowy T, Mrowiec K, *et al*. HSF1 Can Prevent Inflammation following Heat Shock by Inhibiting the Excessive Activation of the *ATF3* and *JUN*&*FOS* Genes. Cells. 2022; 11: 2510.

[13] Shang L, Wang L, Shi X, Wang N, Zhao L, Wang J, *et al*. HMGB1 was negatively regulated by HSF1 and mediated the TLR4/MyD88/NF-κB signal pathway in asthma. Life Sciences. 2020; 241: 117120.

[14] Tang D, Kang R, Zeh HJ, Lotze MT. The multifunctional protein HMGB1: 50 years of discovery. Nature Reviews Immunology. 2023; 23: 824–841.

[15] Yang H, Wang H, Andersson U. Targeting Inflammation Driven by HMGB1. Frontiers in Immunology. 2020; 11: 484.

[16] Tian J, Avalos AM, Mao SY, Chen B, Senthil K, Wu H, *et al*. Toll-like receptor 9-dependent activation by DNA-containing immune complexes is mediated by HMGB1 and RAGE. Nature Immunology. 2007; 8: 487–496.

[17] Leibler C, John S, Elsner RA, Thomas KB, Smita S, Joachim S, *et al*. Genetic dissection of TLR9 reveals complex regulatory and cryptic proinflammatory roles in mouse lupus. Nature Immunology. 2022; 23: 1457–1469.

[18] He Y, Tian W, Zhang M, Qiu H, Li H, Shi X, *et al*. Jieduquyuziyin prescription alleviates SLE complicated by atherosclerosis via promoting cholesterol efflux and suppressing TLR9/MyD88 activation. Journal of Ethnopharmacology. 2023; 309: 116283.

[19] Bamboat ZM, Balachandran VP, Ocuin LM, Obaid H, Plitas G, DeMatteo RP. Toll-like receptor 9 inhibition confers protection from liver ischemia-reperfusion injury. Hepatology (Baltimore, Md.). 2010; 51: 621–632.

[20] Ma X, Liu M. MiR-148b caused liver injury in rats with traumatic hemorrhagic shock by inhibiting SIRT6 expression. Current Molecular Medicine. 2023. (online ahead of print)

[21] Dai W, Wang X, Teng H, Li C, Wang B, Wang J. Celastrol inhibits microglial pyroptosis and attenuates inflammatory reaction in acute spinal cord injury rats. International Immunopharmacology. 2019; 66: 215–223.

[22] Xu S, Qiu Z, Zheng C, Li L, Jiang H, Zhang F, *et al*. Effect of miR-21-3p on lung injury in rats with traumatic hemorrhagic shock resuscitated with sodium bicarbonate Ringer's solution. Annals of Translational Medicine. 2022; 10: 1331.

[23] Livak KJ, Schmittgen TD. Analysis of relative gene expression data using real-time quantitative PCR and the 2(-Delta Delta C(T)) Method. Methods (San Diego, Calif.). 2001; 25: 402–408.

[24] Guan Z, Zhou L, Zhang Y, Zhang Y, Chen H, Shao F. Sulforaphane Ameliorates the Liver Injury of Traumatic Hemorrhagic Shock Rats. The Journal of Surgical Research. 2021; 267: 293–301.

[25] Owattanapanich N, Chittawatanarat K, Benyakorn T, Sirikun J. Risks and benefits of hypotensive resuscitation in patients with traumatic hemorrhagic shock: a meta-analysis. Scandinavian Journal of Trauma, Resuscitation and Emergency Medicine. 2018; 26: 107.

[26] Eastridge BJ, Holcomb JB, Shackelford S. Outcomes of traumatic hemorrhagic shock and the epidemiology of preventable death from injury. Transfusion. 2019; 59: 1423–1428.

[27] Weiss E, Paugam-Burtz C, Jaber S. Shock Etiologies and Fluid Management in Liver Failure. Seminars in Respiratory and Critical Care Medicine. 2018; 39: 538–545.

[28] Wirtz MR, Roelofs JJ, Goslings JC, Juffermans NP. Treatment with ddAVP improves platelet-based coagulation in a rat model of traumatic hemorrhagic shock. Trauma Surgery & Acute Care Open. 2022; 7: e000852.

[29] Khodadadi F, Ketabchi F, Khodabandeh Z, Tavassoli A, Lewis GF, Bahaoddini A. The effect of subdiaphragmatic vagotomy on heart rate variability and lung inflammation in rats with severe hemorrhagic shock. BMC Cardiovascular Disorders. 2022; 22: 181.

[30] Han J, Jia D, Yao H, Lv T, Xu X, Ge X. Cryptotanshinone ameliorates hemorrhagic shock-induced liver injury via activating the Nrf2 signaling pathway. Folia Histochemica et Cytobiologica. 2023; 61: 109–122.

[31] Salem M, Shaheen M, Tabbara A, Borjac J. Saffron extract and crocin exert anti-inflammatory and anti-oxidative effects in a repetitive mild traumatic brain injury mouse model. Scientific Reports. 2022; 12: 5004.

[32] Wang Y, Li C, Gu J, Chen C, Duanmu J, Miao J, *et al*. Celastrol exerts anti-inflammatory effect in liver fibrosis via activation of AMPK-SIRT3 signalling. Journal of Cellular and Molecular Medicine. 2020; 24: 941–953.

[33] Zheng J, Yang N, Wan Y, Cheng W, Zhang G, Yu S, *et al*. Celastrol-loaded biomimetic nanodrug ameliorates APAP-induced liver injury through modulating macrophage polarization. Journal of Molecular Medicine (Berlin, Germany). 2023; 101: 699–716.

[34] Abbas F, Eladl MA, El-Sherbiny M, Abozied N, Nabil A, Mahmoud SM, *et al*. Celastrol and thymoquinone alleviate aluminum chloride-induced neurotoxicity: Behavioral psychomotor performance, neurotransmitter level, oxidative-inflammatory markers, and BDNF expression in rat brain. Biomedicine & Pharmacotherapy. 2022; 151: 113072.

[35] Tong S, Zhang L, Joseph J, Jiang X. Celastrol pretreatment attenuates rat myocardial ischemia/ reperfusion injury by inhibiting high mobility group box 1 protein expression via the PI3K/Akt pathway. Biochemical and Biophysical Research Communications. 2018; 497: 843–849.

[36] Abu Bakar MH, Mohamad Khalid MSF, Nor Shahril NS, Shariff KA, Karunakaran T. Celastrol attenuates high-fructose diet-induced inflammation and insulin resistance via inhibition of 11β-hydroxysteroid dehydrogenase type 1 activity in rat adipose tissues. BioFactors (Oxford, England). 2022; 48: 111–134.

[37] Han LP, Li CJ, Sun B, Xie Y, Guan Y, Ma ZJ, *et al*. Protective Effects of Celastrol on Diabetic Liver Injury via TLR4/MyD88/NF-κB Signaling Pathway in Type 2 Diabetic Rats. Journal of Diabetes Research. 2016; 2016: 2641248.

[38] Xin J, Yang T, Wu X, Wu Y, Liu Y, Liu X, *et al*. Spatial transcriptomics analysis of zone-dependent hepatic ischemia-reperfusion injury murine model. Communications Biology. 2023; 6: 194.

[39] Breternitz W, Sandkühler F, Grohmann F, Hampe J, Brosch M, Herrmann A, *et al*. The HSF1-CPT1a Pathway Is Differentially Regulated in NAFLD Progression. Cells. 2022; 11: 3504.

[40] Jin Y, Li C, Xu D, Zhu J, Wei S, Zhong A, *et al*. Jagged1-mediated myeloid Notch1 signaling activates HSF1/Snail and controls NLRP3 inflammasome activation in liver inflammatory injury. Cellular & Molecular Immunology. 2020; 17: 1245–1256.

[41] Qiao Y, Zhang X, Zhao G, Liu Z, Yu M, Fang Z, *et al*. Hepatocellular iNOS protects liver from ischemia/reperfusion injury through HSF1-dependent activation of HSP70. Biochemical and Biophysical Research Communications. 2019; 512: 882–888.

[42] Han SJ, Kim M, Novitsky E, D'Agati V, Lee HT. Intestinal TLR9 deficiency exacerbates hepatic IR injury via altered intestinal inflammation and short-chain fatty acid synthesis. The FASEB Journal. 2020; 34: 12083–12099.

[43] Hao L, Zhong W, Sun X, Zhou Z. TLR9 Signaling Protects Alcohol-Induced Hepatic Oxidative Stress but Worsens Liver Inflammation in Mice. Frontiers in Pharmacology. 2021; 12: 709002.

[44] Chen SN, Tan Y, Xiao XC, Li Q, Wu Q, Peng YY, *et al*. Deletion of TLR4 attenuates lipopolysaccharide-induced acute liver injury by inhibiting inflammation and apoptosis. Acta Pharmacologica Sinica. 2021; 42: 1610–1619.

[45] Shi P, Zhu W, Fu J, Liang A, Zheng T, Wen Z, *et al*. Avicularin alleviates acute liver failure by regulation of the TLR4/MyD88/NF-κB and Nrf2/HO-1/GPX4 pathways to reduce inflammation and ferroptosis. Journal of Cellular and Molecular Medicine. 2023; 27: 3326–3338.

[46] Sosa RA, Terry AQ, Ito T, Naini BV, Zheng Y, Pickering H, *et al*. Immune Features of Disparate Liver Transplant Outcomes in Female Hispanics With Nonalcoholic Steatohepatitis. Transplantation Direct. 2023; 9: e1550.

[47] Ma L, Geng J, Chen W, Qin M, Wang L, Zeng Y. Effects of TLR9/NF-κB on oxidative stress and inflammation in IPEC-J2 cells. Genes & Genomics. 2022; 44: 1149–1158.

[48] Li S, Feng G, Zhang M, Zhang X, Lu J, Feng C, *et al*. Oxymatrine attenuates TNBS-induced colinutis in rats through TLR9/Myd88/NF-κB signal pathway. Human & Experimental Toxicology. 2022; 41: 9603271221078866.

[49] Li J, Liu Y, Duan P, Yu R, Gu Z, Li L, *et al*. NF κB regulates HSF1 and c Jun activation in heat stress induced intestinal epithelial cell apoptosis. Molecular Medicine Reports. 2018; 17: 3388–3396.